ARCHIVES
Of
FOUNDRY ENGINEERING

Published quarterly as the organ of the Foundry Commission of the Polish Academy of Sciences

ISSN (1897-3310)
Volume 11
Special Issue
2/2011
143–148

28/2

Grain size reduction in the 713C nickel superalloy as a result of heat treatment

M.B. Lachowicz [a], M. Faryna, [b] M. Podrez-Radziszewska[a],
[a] Wroclaw University of Technology, Institute of Materials Science and Applied Mechanics, Smoluchowskiego 25, 50-370 Wroclaw, Poland
[b] Institute of Metallurgy and Materials Science Polish Academy of Science Cracow, Poland
*Corresponding author. E-mail address: maciej.lachowicz@pwr.wroc.pl

Received 11.04.2011; Approved for print on: 26.04.2011

Abstract

The paper presents metallographic test results for the 713C nickel superalloy after heat treatment and crystallographic orientation analysis performed with the EBSD method. The 713C alloy was subjected to annealing in the temperature of 950 ^{o}C for 30 hours followed by air-cooling. As a result of the applied heat treatment the local grain size reduction in the alloy was observed. It has been found that in the primary grains the new subgrains of different crystallographic orientation are created. Between the new grains and the primary grains the boundaries of high angle appear. Orientation change in the micro-areas is closely related to the carbides rebuilding and volume diffusion of elements dissolved in the γ - γ' alloy matrix and the (NbTi)C carbides.

Keywords: heat treatment, metallography, superalloy 713C, Ni_3Al, NbC, EBSD

1. Introduction

The nickel Inconel 713C superalloy belongs to the group of casting alloys based at the austenite γ matrix strengthened with the Ni_3AlTi - γ' intermetallic phase. Most frequently the 713C alloy is applied in the directly after casting state. However, it could also be subjected to heat treatment consisting in solutioning within the temperature range from 1150 ^{o}C to 1180 ^{o}C for 2 to 4 h, followed by ageing in temperature of 950 ^{o}C for 4 to 100h [1]. In case of the 713C alloy the stress relief annealing in temperatures of 1200 ^{o}C and 1230 ^{o}C [2] is also frequently applied. Cooling may be conducted in furnace, air or water.

Good mechanical properties of the nickel superalloys in the increased temperature are the result of their chemical composition, type, morphology, quantity and distribution of the intermetallic phases, as well as the heat treatment technology. Increase in the γ' phase share in the alloys structure result in the growth in cracking stress by some 200 MPa in temperatures above 700^{o}C, and radical growth in the creep strength. In the conventional nickel superalloys the creep resistance is being achieved by diminishing the grain boundaries surface and lowering the stacking fault energy through molybdenum and wolfram dissolution in the γ austenite. In the newly developed monocrystallic alloys the increase in strength properties is being obtained by increasing the quantity of γ' precipitations to 70 – 75% and total elimination of grain boundaries. In the conventional alloy grade 738, the content of γ' phase amounts to 45%, in the directionally crystallised alloy grade 729 - 60%, and in the monocrystallic alloy grade CMSX-4 the share of γ' phase amounts to 75% [3,4]. The Inconel 713C alloy contains about 50% of the γ' phase, with particle size from 0,4 to 1μm [1,5,6]. According to our own research the quantity of particles significantly exceeds 50% [7,8,9]. Precipitations of γ' smaller than 0,4 μm are obtained on trial in the 713C alloy in the continuous casting process of ingots with rather small diameters of 10 mm at the high cooling rates. However, the strong transcrystallisation and segregation of the chemical composition appears then, as well as the continuous reticular precipitation of carbides and the γ-MC eutectic areas [5]. In the works [10-12] Bińczyk and Śleziona focused on the primary grain size reduction through modification of the casting parameters. This caused also improvement in the alloy mechanical properties and its plasticity. However, it is to be supposed that grain size reduction may cause a drop in creep strength, though the grain size reduction may also be very advantageous from the other alloy applications point of view.

In the trials of surfacing and welding of the 713C superalloy a heat treatment was applied after welding, in order to limit the alloy cracking, as well as microstructure homogenising and obtaining the assumed mechanical properties. During the heat treatment, creation of precipitations assuming the lattice morphology between carbides was frequently observed. The created precipitations resulted from diffusive decomposition of carbides. The issue has been discussed in works [9,13], where the stoichiometric formula has been assigned to the precipitations of $Ni_3(Al,Ti,Nb)C$ and $Ni_3(Al,Ti,Nb)$.

The post-carbide precipitation lattice with its morphology resembles grains, and the microstructure with its character resembles the material processed plastically and subjected to recrystallisation rather, than the cast one. Exemplary microstructure obtained after the heat treatment has been described in works [9,13] and presented in Fig. 1. While analysing the microstructure inside grains created through precipitation, one may have the impression that orientation and morphology of the γ' particles inside is different from that in the remaining area. Such areas – grains are indicated in Fig. 1 with arrows. Fig. 2 and 3 present magnified fragment of the microstructure, where precipitations of the γ' phase of the parallelogram shape with clearly different orientation inside grain may be seen.

If inside the created area, limited only with the post-carbide precipitation, the different orientation of the γ' phase appears, this could give the evidence of its different crystallographic orientation. Considering the fact that the γ' phase is coherent with the γ austenite, its orientation is closely related to the austenite orientation. Different orientation of the γ' phase inside the created area could testify for another, new grain appearance in this place, and as a result of the heat treatment the grain size reduction follows.

2. Material and research methodology

In the tests the Inconel 713C alloy of the following chemical composition was used: 12.8 % Cr, 4.15 % Mo, 1.73 % Nb, 6.2 % Al, 1.04 % Ti, 0.12 % C, 0.017 % B, 5 ppm Zr, 0.19 % Fe, Ni – the rest. For the tests the specimens of the 120 x 70 x 5 mm size were cast into the ceramic form, from which the samples of the 10x60mm size for the metallographic tests were made.

Before heat treatment the samples were grinded to the thickness of 4mm. Next, a metallographic section was made at one of its surfaces, and the primary grain size, typical for the 713C alloy - from several to over ten millimetres - was estimated.

Subsequently, the samples were subjected to heat treatment, consisting in annealing in the temperature of 950 ^{o}C in the atmosphere of argon for 30h, and then cooled in the air.

Metallographic section after heat treatment was performed at the same surface as before it. The surface was subjected only to paper grinding and electrolytic polishing in order to eliminate the first and second order stresses, which disturb the diffraction image. After the heat treatment the sample was grinded for not more than 0,05 mm, only to remove the superficial tarnish. Microstructure observation, exactly at the same surface as before the heat treatment, only after its slight grinding was necessary for avoiding the observation of other grains with different crystallographic orientation, or the same grains but in the other cross-section.

Aim of the study was confirmation whether the new sub-grains are really being created in the alloy microstructure as a result of heat treatment and whether the different orientation of the γ' particles is only a subjective impression.

For crystallographic orientation evaluating the EBSD (electron backscatter diffraction) technique was used. The tests were performed in the Institute of Metallurgy and Materials Science of Polish Academy of Science in Cracow, using the Philips XL 30 ESEM scanning electron microscope, equipped with the EBSD Chanel 5 system from Oxford Instruments [14,15].

Electron diffractions were solved with consideration for the austenite γ lattice parameters.

Effect of the research was creation of crystallographic orientation maps in the Euler angle orientation, the crystallographic orientation indexes and the misorientation angles between grains. Misorientation profiles between grains were also performed. Maps of the orientation distribution were made at a scanning pitch of 1μm and 2μm. Microscopic tests were performed using the light and scanning electron microscopy. The JEOL JSM-5800LV-Oxford LINK ISIS-300 microscope was used. The samples were etched with ML3 [7,8].

3. Test results

3.1. Crystallographic orientation microscopy

As a result of the research conducted with use of the EBSD method it has been found that in the areas of precipitation lattice appearance of the phase created from carbides decomposition, the new grains of different crystallographic orientation are being created. That way the grain size reduction is following. Grains in the material before heat treatment were of the several to over ten millimeters in size. After the heat treatment, new grains with high-angle boundaries were created within the primary grains. Thus, these are not the small crystallographic orientation fluctuation areas but the grains of misorientation angles of over 10^{o}, so the high angle boundary is being created.

That is as much interesting, because the heat treatment was applied to the cast material, in which no recrystallisation after cold work appears, as happens in case of the materials processed plastically, and which in the heat treatment temperature should not undergo any mass phase transition. It results from observation of the ATD and DSC thermal analysis curves that in the temperature of about 950^{o}C no mass transitions occur [16-18].

Exemplary image of the alloy microstructure, in place where one of the maps with crystallographic orientation distribution was made, has been shown in Fig. 4, whereas the Fig. 5 shows the orientation distribution map in the Euler angle arrangement, and Fig. 6 presents distribution of the grain boundaries determined at the base of misorientation angle.

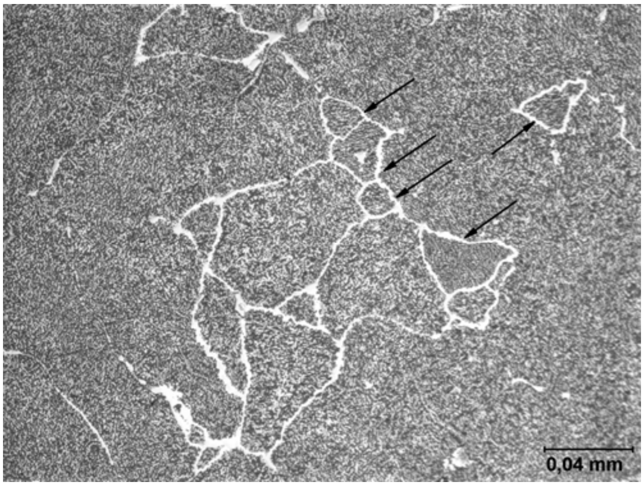

Fig. 1. Microstructure of the 713C alloy after heat treatment. Visible subgrains with bright precipitations of the phase created during carbides decomposition at the subgrain boundaries. Arrows indicate areas of different orientation of the γ' phase. Etched with ML3.

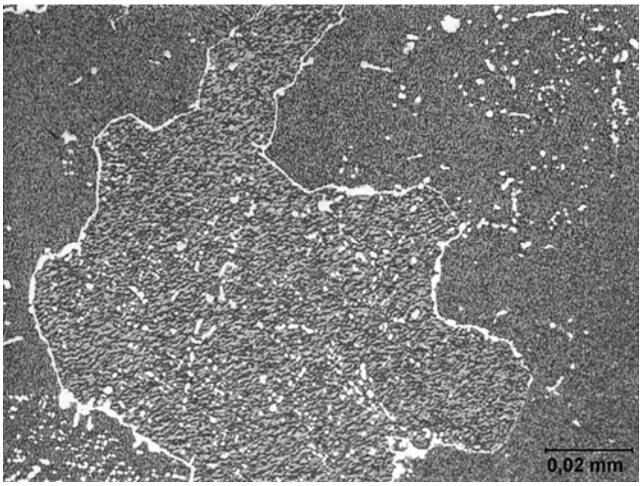

Fig. 2. Magnified image of an exemplary subgrain. Visible different orientation of the γ' phase inside and outside of the grain, as well as the bright phase precipitations created from carbides decomposition. Etched with ML3.

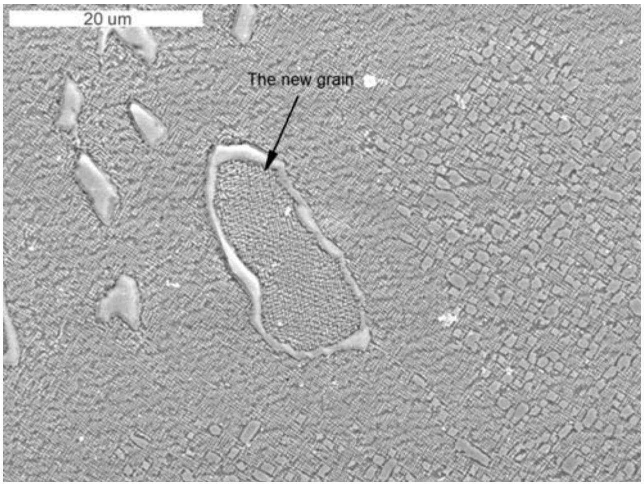

Fig. 3. Subgrain created during heat treatment with the different γ' phase morphology visible inside the subgrain. Etched with ML3. SEM.

In the EBSD method the areas of different orientation are distinguished by different colours, according to the international crystallographic orientation indexing (the so called basic triangle). According to that, the red colour, for example corresponds to the orientation <001>, blue to <111>, and green to <101>. Other colours, which are the superposition of the basic colours, determine the intermediate directions. Considering the necessity of furnishing the work with black and white drawings, the new grains, their orientations, as well as boundaries have been described symbolically at the drawings and in the text. Marking the grains and their borders with shadows of gray only is insufficient for their unique representation.

Figure 4 presents the image of microstructure observed in the non-etched state. Visible are two primary grains present in the alloy after casting with orientations similar to [101] – grain No 1 and [111] – grain No. 2. Boundary between the two grains has also been shown. The arrows indicate new grains created as a result of heat treatment. Figure 5 shows the same area of microstructure as in Fig. 4, with the crystallographic orientation distribution map made in the Euler angle arrangement. Exemplary grain orientations have been mapped here, which could be read directly from the basic triangle. Colour indexing has been matched from the map of orientation distribution in the IPF (index pole figure) arrangement shown in Fig. 6. Crystallographic direction indices were introduced to Fig. 4 on purpose, for better legibility of both maps. In Figure 6 with the IPF map, grain boundaries marked with symbols (DG1,2,3,4) and arranged according to the misorientation angle were additionally introduced.

The following markings for boundary types, depending on the misorientation angle, have been assumed:

No marking – angle 2-15^{o}, e.g. grains G1 and G2 in Fig. 5.
DG1 – angle 15 – 25^{o}
DG2 – angle 25 – 35^{o}
DG3 – angle 35 – 45^{o}
DG4 – angle 45 – 55^{o}

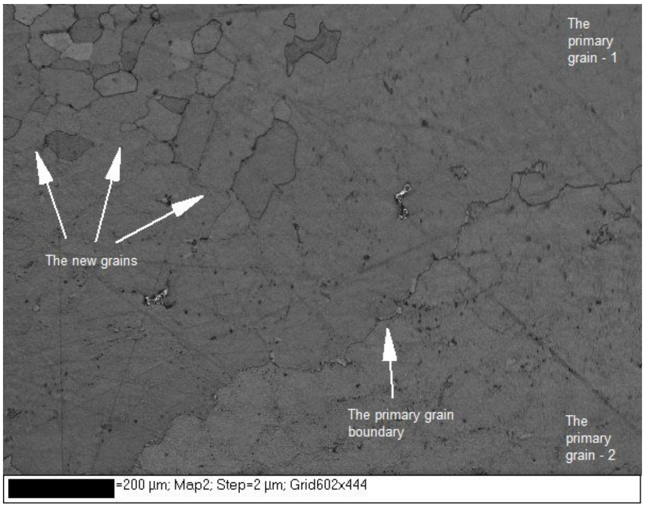

Fig. 4. Alloy microstructure image in place where crystallographic orientation distribution maps have been made. Visible grain boundaries of the primary and newly created grains. Non-etched state. SEM, SE.

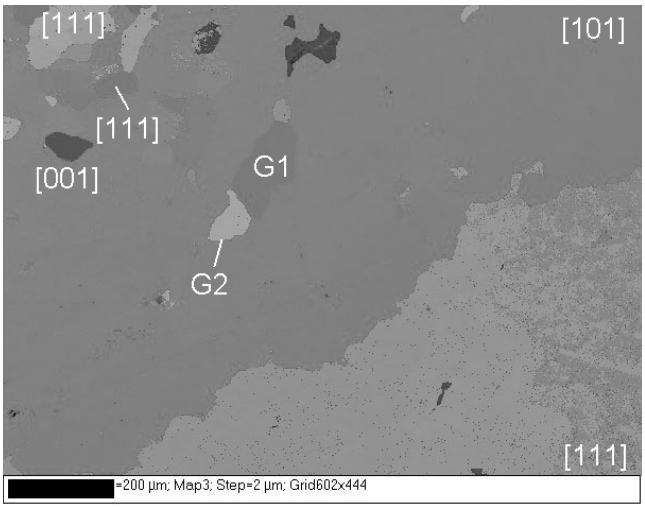

Fig. 5. Orientation distribution map in the Euler angle arrangement. Crystallographic orientation has been mapped for some grains, which could be directly read from indexing at the basic triangle. SEM, EBSD.

While analysing the orientation change it seems that it probably runs, first of all, through small crystallographic orientation fluctuation with misorientation angle of 3-5^{o}, and next the micro-area of misorientation angles much bigger than 15^{o} is being created. The conclusion is confirmed by observations at the orientation maps of the areas with different shade than that of the matrix, where misorientation angles of 2 to 15^{o} were present. Such areas are marked in Fig. 5 as G1 and G2. As a result of the

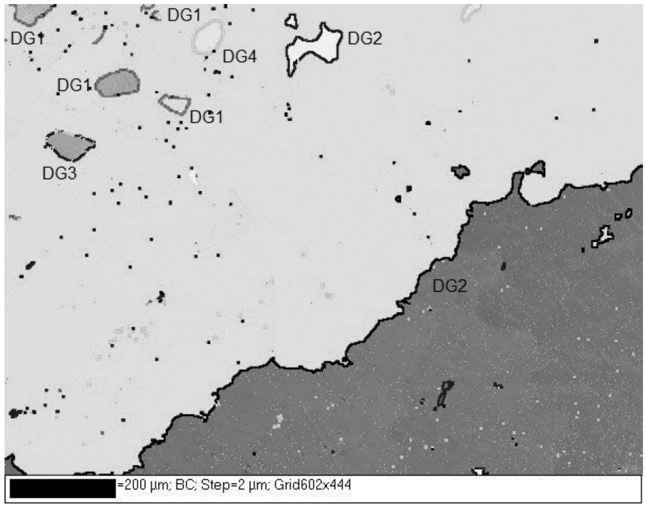

Fig. 6. Orientation distribution map in the IPF arrangement, with the mapped grain boundaries determined in relation to the misorientation angle. SEM, EBSD.

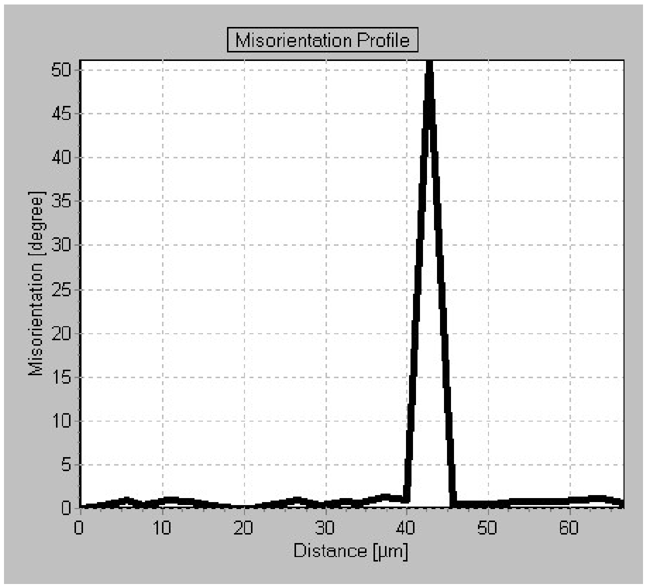

Fig. 7. Exemplary profile of misorientation angle performed along the straight line between grains with the DG4 boundary (Fig.6), and the primary grain No. 1 (Fig.4). EBSD.

observation it could be noted, that shape of those areas indicate that they are also grains. At the map with Euler angle arrangement the grains are well visible despite the drawing of grey shades. They could also be observed in the alloy microstructure shown in Fig. 4. At the IPF orientation map in Fig. 6, their outline is not well visible yet, because the areas of orientation close to [101] assume the green colour and its shades are poorly visible when converted to grey shades.

Orientation change in the micro areas has to be influenced by rebuilding of primary carbides, as creation of the new subgrain was observed only in the areas limited by the post-carbide precipitations lattice. Probably the orientation change in the micro areas will be related to volumetric diffusion of elements dissolved in the alloy matrix, that is the γ and γ' phases and carbides of the (NbTi)C type. At that study stage it is not possible to determine how the diffusion fluxes will run, however it seems that the orientation change could be the derivative of the diffusion fluxes of elements dissolved in the matrix and in the carbides. The issue is a complex one, as the physical system involves many variables: matrix – dispersion particle γ' and the (NbTi)C carbide, as well as several elements, which could simultaneously diffuse, e.g. Al, Ni, Ti between austenite γ and the γ' phase, Ti, Nb, Mo, Cr and C, at the same time between carbide, γ and γ'.

The phenomenon of carbides decomposition and creation of new grains could be considered in a different way. Carbides decomposition and precipitation of new phases could be the result – the sequence of the high-angle boundary creation. It is well known, that grain boundaries are the places where precipitation processes happen most easily. This results from high density of defects – saturation with vacancies and the dislocations pile-up. That way the elements diffusion and new phase nucleation is facilitated. Thus, it is not excluded, that just in the first place, the crystallographic orientation change in the micro areas of matrix takes place, and next the grain boundary is created, and that is the reason for diffusive carbides decomposition and new phases precipitation at the new boundaries.

4. Summary

1. Heat treatment was applied to the cast material, which should not undergo phase transition in the temperature of 950^0C.
2. Heat treatment with the set parameters leads to local grain size reduction.
3. As a result of the heat treatment, in the area of primary grains the new grains with different crystallographic orientation were created. Boundaries of the newly created grains are the high-angle boundaries.
4. Orientation change in micro areas is closely related to the carbides rebuilding and volumetric diffusion of elements dissolved in the γ - γ' alloy matrix and the (NbTi)C type carbides.
5. It is very probable that, in the first place, the new grains are being created in the alloy, at the boundaries of which the phases created from carbides rebuilding are precipitating. The high-angle grain boundaries facilitate diffusion of the alloy constituents.

It is interesting to know whether extending of the treatment periods will lead to grain size reduction in the whole volume and how it would impact the alloy properties. According to the Hall-Petch rule regarding the mechanical properties an increase in the alloy strength should follow. However, for the heat-resisting alloy the grain size reduction causes a drop in the creep resistance. The discussed topic is still interesting from the transition physics point of view.

Acknowledgements

The research was conducted as part of a programme - Fellowship co-financed by the European Union within the European Social Fund: Human Capital Operational Programme, Subactivity 4.1.1: Consolidation and development of the didactic potential of the university. Development of the didactic and scientific potential in young academic personnel of the Wroclaw University of Technology, Edition III – 10.2010 – 03.2011.

Bibliography

[1] A. Somoza, G. Santos, A. Ges, R. Versaci, F. Plazaola, Age-hardening and precipitation phenomena in the Inconel 713C superalloy studied by means of positron lifetime spectroscopy, Phys. Stat. Sol. 174, (1999) 189-198.

[2] B. Mikułowski; Heat-resisting and creep-resisting alloys – superalloys; AGH, Kraków, 1997 (in Polish).

[3] D Danciu, B. Dubiel, H.J Penkalla, F. Schubert, A. Czyrska-Filemonowicz, The microstructure of single crystal nickel-base superalloys for advanced industrial gas turbine components, Inżynieria Materiałowa 4 (2001) 274-277.

[4] C.N. Panagopoulos, K.I. Giannakopoulos, V. Saltas, Wear behavior of nickel superalloy, CMSX-186, Materials Letters 57 (2003) 4611-4616.

[5] F. Zupanič, T. Bončina, A. Križman, F.D. Tichelaar, Structure of continuously cast Ni-based superalloy Inconel 713C, J Alloys Compo 329, (2001) 290-297.

[6] C.N. Wei, H.Y. Bor, C.Y. Ma, T.S. Lee, A study of IN-713LC superalloy grain refinement effects on microstructure and tensile properties, Materials Chemistry and Physics 80 (2003) 89-93.

[7] M. Lachowicz, W. Dudziński, K. Haimann, M. Podrez-Radziszewska, Microstructure transformations and cracking in the matrix of γ-γ' superalloy Inconel 713C melted with electron beam, Mat Sci Eng A 479 (2008) 269-276.

[8] M. Lachowicz, W. Dudziński, M. Podrez-Radziszewska, TEM observation of the heat-affected zone in electron beam welded superalloy Inconel 713C, Mater Charact 59 (2008) 560-566.

[9] M. Lachowicz, W. Dudziński, Non-equilibrium decomposition of MC carbides in superalloy Inconel 713C melted with welding techniques, Archiv Metall Mater, vol.55, No 1 (2010) 305-315.

[10] F. Bińczyk, J. Śleziona, Effect of modification on the mechanical properties of In-713C alloy. Arch of Found Eng 1 vol 10 (2010) 195-198.

[11] F. Bińczyk, J. Śleziona, Macro- and microhardness of In-713C nickel superalloy constituents, Arch of Found Eng 4 vol 9 (2009) 9-12.

[12] F. Bińczyk, J. Śleziona, T. Mikuszewski, Effect of repeated remelting on the chemical composition and structure of nickel alloys, Arch of Found Eng 1 vol 10 (2010) 189-194.

[13] Lachowicz Maciej. Microstructural changes in padding welds made from the 713C alloy after heat treatment. Arch of Found Eng 3 vol 10 (2010).

[14] M. Faryna, Dyfrakcja elektronów wstecznie rozproszonych – kilka uwag praktycznych, Inżynieria Materiałowa 1 (2009) 5-11 (in Polish).
[15] M. Faryna, Dyfrakcja elektronów wstecznie rozproszonych – kilka uwag teoretycznych, Inżynieria Materiałowa 4 (2009) (in Polish).
[16] F. Bińczyk, J. Śleziona, R. Przeliorz, Calorimetric examination of mixtures for modification of nickel and cobalt superalloys, Arch of Found Eng 2 vol 9 (2009) 97-100.
[17] F. Bińczyk, J. Śleziona, Phase transformations and microstructure of In-713C nickel superalloy, Arch of Found Eng 2 vol 9 (2009) 109-112.
[18] F. Bińczyk, J. Śleziona, J. Cwajna, S. Roskosz, ATD and DSC analyses of nickel superalloys, Arch of Found Eng 3 vol 8 (2008) 5-8.